

Spatial evolution of tumors with successive driver mutationsTibor Antal,¹ P. L. Krapivsky,² and M. A. Nowak³¹*School of Mathematics, Edinburgh University, Edinburgh EH9 3FD, United Kingdom*²*Department of Physics, Boston University, Boston, Massachusetts 02215, USA*³*Program for Evolutionary Dynamics, Department of Mathematics, and Department of Organismic and Evolutionary Biology, Harvard University, Cambridge, Massachusetts 02138, USA*

(Received 15 April 2015; published 12 August 2015)

We study the influence of driver mutations on the spatial evolutionary dynamics of solid tumors. We start with a cancer clone that expands uniformly in three dimensions giving rise to a spherical shape. We assume that cell division occurs on the surface of the growing tumor. Each cell division has a chance to give rise to a mutation that activates an additional driver gene. The resulting clone has an enhanced growth rate, which generates a local ensemble of faster growing cells, thereby distorting the spherical shape of the tumor. We derive formulas for the abundance and diversity of additional driver mutations as function of time. Our model is semi-deterministic: the spatial growth of cancer clones is deterministic, while mutants arise stochastically.

DOI: [10.1103/PhysRevE.92.022705](https://doi.org/10.1103/PhysRevE.92.022705)

PACS number(s): 87.10.Mn, 02.50.Ey, 87.19.xj

I. INTRODUCTION

Cancer arises when somatic cells receive multiple mutations that enhance their net reproductive rate [1,2]. Tumors contain 35 to 70 genetic alterations that change protein sequences [3]. The vast majority of those mutations are passengers that do not confer a selective growth advantage. A small subset, however, are driver mutations that promote tumorigenesis. In the human genome about 135 genes are known that can function as drivers when mutated (either by point mutation, insertion, deletion, or amplification). Driver mutations affect pathways that regulate cell survival, proliferation and genome maintenance. Any tumor contains between 2 to 8 driver mutations [3]. In this paper we study the accumulation of such drivers in a spatial model of tumor growth.

Mathematical modeling of cancer evolution is a rapidly developing field [4]. Cancer is a multi-facet phenomenon and many features need to be addressed in modeling. The age incidence of cancers [5], the effect of tissue geometry and chromosomal instability on cancer initiation [6,7], the inactivation of tumor suppressor genes [8], the accumulation of driver and passenger mutations in expanding tumors [9–12], the molecular clock of cancer [13], and the emergence of resistance to cancer therapy [14–18] are some of the issues that have been studied.

Modeling the evolution of cancer has been mostly performed in the homogeneous setting [4,19] which is an obvious idealization, especially for solid tumors. The homogeneous setting allows to focus on the temporal dynamics and provides a useful theoretical laboratory to probe the efficacy of drug combinations. A more faithful spatial modeling is necessary [20–22] for understanding tumor invasion and metastasis [23], and effort in this direction is growing. Previous spatial models mainly focus on the evolution of already existing types of cells in space. Most models are either continuum mathematical models based on partial differential equations [21,22,24] or discrete cell population models using cellular automata-type computer simulations [25]. Simulations are often performed at cell levels, incorporating cell movement and different cell types, and are either lattice based or off-lattice [22,25,26]. One of the challenges in the modeling using partial differential

equations governing densities of different cell types is that the boundary of the tumor is also evolving (free boundary problem) [24,27–29].

Here we develop a geometric approach for the accumulation of driver mutations in spatially expanding tumors. The spatial inhomogeneity of tumors and the spatial distribution of genetic mutations have been studied in recent experimental and theoretical works [13,30]. Since different mutations are present in different spatial regions of the tumor, spatial inhomogeneity is relevant for choosing the optimal targeted drug therapy for patients. In this paper we focus on the evolving shape of the tumor and its interplay with the onset of successive driver mutations. We deliberately simplify the model as much as possible, while keeping the key features, namely the spatial growth and the competition between different mutants. The goal is to eventually apply spatial tumor modeling of the accumulation of driver mutations to problems which were recently analyzed in the idealized ‘mean-field’ framework of well mixed population of cells (see, e.g., [9,10,31–34]), as well as to other problems which can only be formulated in the spatial framework.

Our model is reminiscent of the pioneering lattice model of cancer which incorporates mutation [35–37]. In contrast to this earlier work, we assume that mutations occur only on the surface of the growing tumor. Furthermore, we assume that the spatial expansion is deterministic. Only mutational events are stochastic. We also mention a few more recent related studies. In Ref. [38], the accumulation of many successive driver mutations was studied by computer simulations on a two-dimensional lattice. It was found that space makes the arrival of new driver mutations slower than in a well-mixed population. Since including both space and mutation make models quite complex, one usually resorts to simulations and to approximate treatments [39,40]. Analytical results have been established in a few simple situations, e.g., for the one-dimensional tissue geometry [17,41,42] and in arbitrary dimension in the case of the accumulation of neutral mutations [43].

Our model has two basic ingredients: stochastic nucleation of new mutants and deterministic growth of existing cell types. Nucleation and growth are ubiquitous natural phenomena, and

our model overlaps with classical models of such processes. One example is a polynuclear growth model (see [44] for a review). Similar models have been used in cosmology (see [45] for a review). The contrasting features of our model is the nucleation on the surface of the growing tumor and differences in the growth rates; in other applications nucleation events usually happen in the bulk and growth rates are equal. For example, in cosmological applications [45] cosmic bubbles grow at a speed of light. In our model a mutation activating a driver gene leads to enhanced growth rate leading to the distortion of the spherical shape of the original tumor. Nucleation and growth processes with different growth rates have been studied in [46,47]. Similar modeling has been in the context of expanding bacterial colonies [48], particularly in modeling of selective sweeps in growing microbial colonies. Our model is mathematically the same as the one proposed in that latter context in Ref. [49] and studied in details in Ref. [50]. The experimental setting [48–50], as well as numerical [48] and theoretical [50] analyses were two-dimensional. Our focus is on three dimensions and our main findings are related to probabilistic aspects.

We analyze in detail the simplest case of the competition between the original cancer clone and one mutant clone. We describe the boundary separating the clones, determine the time when the mutant clone envelopes the original cancer clone which thereby ceases to grow any further, and compute the probability that it happens before the arrival of any other mutant clone.

Our model is a step toward understanding the three-dimensional growth dynamics of cancer. In particular, our aim is to study how the growth pattern is influenced by driver mutations that lead to faster growth thereby distorting the basic shape of the tumor. Experimental applications include the spatial genetic analysis of primary tumors [13] or the growth of spheroids and organoids in laboratory settings [51,52].

II. THE MODEL

In our model, cells only proliferate on the surface of the tumor. Inside the tumor, cells are non-dividing, hence there are no evolutionary dynamics there. This assumption is plausible for early stages of tumor progression, where only tumor cells close to the surface can get enough oxygen or other nutrition to divide. A typical tumor developing in vivo has most of its cell proliferation constrained to the border [53–55], which suggests that cell surface diffusion is the main mechanism responsible for growth in any type of tumor. At later stages of tumor progression, when angiogenesis starts to work, this assumption may no longer be valid, but there can always be interior regions with low supply of nutrients and oxygen and low activity of cell division.

The dynamics of our model is governed by two rates. The first represents the rate at which the surface of the tumor advances in the direction orthogonal to the surface. The second is the rate at which new driver mutations occur on the surface. Without mutations, the original tumor grows spherically [55–57]. Since cell divisions only occur on the surface of the tumor, mutations can occur only there, at a constant rate per unit surface area and unit time. We include in this mutation rate the survival probability of mutant clones. In

other words, we are only tracking mutants that survive. Since we assume that these mutants have selective advantage over the original tumor, the mutant clones keep spreading. A more comprehensive consideration tracking all mutants including those that quickly disappear is necessarily based on stochastic growth [58].

We set both the speed of the original tumor growth and the mutation rate to unity. This can always be done by appropriately choosing the units of length and time. If no mutation has happened up to time t , the original tumor is a growing ball during this time interval and with our convention about the speed its radius is t at time t . The appearance of mutants changes this simple pattern since the part of the surface that belongs to a mutant grows with a larger speed. The surface of the tumor still grows in the normal direction but the competition between mutants and the original tumor, and also between different mutants once they touch, affects the surface.

We focus on the biologically most relevant three-dimensional case, but we also present a few basic results for two dimensions. In analytical work, we limit ourselves to the simplest case of two types of cells: (i) the initiating cancer cell with growth rate one; and (ii) a mutant cancer cell with growth rate $v > 1$. The mutant cell arises by activation of an additional driver. The surface of the tumor either belongs to a mutant clone or the original tumor. A point at a distance dt from the surface of the tumor will be occupied by a mutant clone dt times later, if a mutant can reach that point earlier than a non-mutant (see a more detailed description later). A mutant clone advances a distance vdt and a point at the surface will be occupied by a mutant if there is a mutant clone on the surface within a distance βdt , with $\beta = \sqrt{v^2 - 1}$. Hence the relative area of the surface which is covered by mutant is expanding, with the boundary moving at constant speed β , see [49,50].

The simplicity of the model is manifested by its dependence on a single dimension-less parameter v . We have achieved this by rescaling the length scale and the time scale. (The dependence of the results on the detailed parameters is discussed in Sec. V).

III. SINGLE MUTANT CLONE

In this section we investigate the interaction between the original tumor and a single mutant clone. The original tumor begins to grow at time $t = 0$ at the origin. Without loss of generality we can choose $t = 1$ as the birth time of the mutant clone. At this point the original tumor is a ball of radius one around the origin. We choose the coordinate system in such a way that $(x, y, z) = (1, 0, 0)$ is the seed of the mutant clone. Since we do not consider other birth events, the tumor remains rotationally symmetric around the x axes and we can focus on a two-dimensional cut through the (x, y) plane. [For a mutant clone initiated at spherical coordinates (r_0, θ_0, ϕ_0) the shape is the same as the one initiated at $(r_0 = 1, \theta_0 = 0, \phi_0 = 0)$, with both space and time stretched by r_0 supplemented by rotation θ_0, ϕ_0].

A two-dimensional cut of a single mutant clone is depicted in Fig. 1. Figure 1 shows that the original tumor grows up to a capture time t_c , and it ceases to grow for $t > t_c$. The final

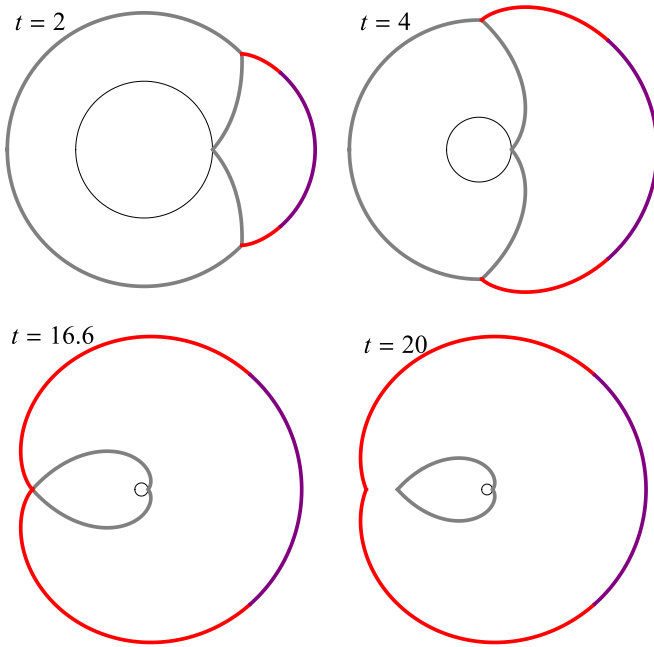


FIG. 1. (Color online) Slices of a tumor with a single mutant clone at times $t = 2, 4, 16.6, 20$. The original tumor is initiated at the origin, and the mutant is initiated at $t = 1$ at $(1, 0, 0)$ and has fitness $v = 1.5$. The tumor at the initiation time is drawn as a thin line at each stage to show the length scale. The boundaries of the original tumor are depicted by thick lines emanating from $(1, 0)$, other thick lines represent the outer boundary of the mutant clone. The central part and the side parts of the outer boundary of the mutant clone are described by different functional forms. On the lower left picture the original tumor is just captured by the mutant clone, this happens at $t_c = e^{\pi/\beta} = 16.6087 \dots$; on the lower right one the mutant overgrows the enclosed original tumor.

“barnacle” shapes of the original tumor are shown on Fig. 2. The shapes shown on these figures were previously found by numerical [48] and analytical [49,50] means in analyses of growing microbial colonies. More general shapes arise in the context of nucleation and growth [46]; in our language they correspond to the situation when the mutant is initiated away from the surface. We briefly re-derive these results as we

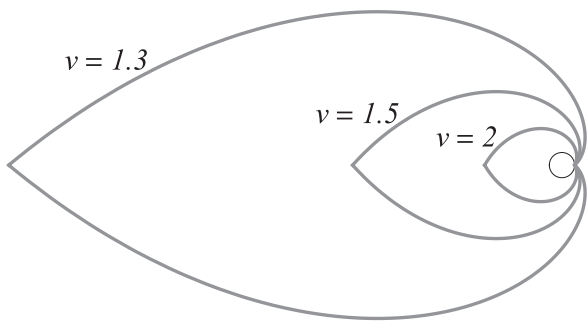


FIG. 2. The final barnacle shape of the original tumor after it has been captured by the mutant clone. Shown results corresponds to the fitness values $v = 1.3, 1.5, 2$. The mutant is always initiated at $t = 1$, and the capture takes place at $t_c = e^{\pi/\beta} = 43.9052, 16.6087, 6.13371$, respectively, for the illustrated fitness values. The circle represents the original tumor at the initiation time $t = 1$ of the mutant clone.

use them to compute the final volume of the original tumor; we shall also need these results in the next section.

In the two-dimensional cut through the (x, y) plane, Fig. 1, the shape of the original tumor at time t has generally two parts. The first is the inner boundary between the original tumor and the mutant, which in polar coordinates is $r(\theta) = e^{\theta/\beta}$. In Cartesian coordinates,

$$x(\theta) = e^{\theta/\beta} \cos \theta, \quad y(\theta) = e^{\theta/\beta} \sin \theta. \quad (1)$$

This is valid when $0 \leq \theta \leq \theta_0$, where

$$\theta_0 = \beta \log t. \quad (2)$$

For $\theta > \theta_0$, the surface of the original tumor has not yet been affected by the mutant, so it is a sphere of radius t around the origin. Note that the above curve (1) is known as the logarithmic spiral. It was already studied by Descartes and Jacob Bernoulli, and it appears in numerous contexts ranging from the Nautilus shell and insect flights [59] to nucleation-and-growth processes [46] and bacterial growth [48–50].

The part of the original tumor which has not been affected by the interaction with mutant clone lies in the angular region $\theta_0 \leq \theta \leq \pi$. When θ_0 becomes equal to π , the original tumor is completely covered by the mutant. This happens at time

$$t_c = e^{\pi/\beta}. \quad (3)$$

After this time the original tumor ceases to grow any further, and its final volume is

$$V_c(\beta) = \frac{2\pi}{3} \frac{\beta^2}{\beta^2 + 9} (1 + e^{3\pi/\beta}). \quad (4)$$

The mutant at time t is separated from the original tumor by the inner boundary (1). The outer boundary of the mutant consists of two parts. The middle part is a sphere around $(1, 0)$ with radius $v(t - 1)$:

$$\begin{aligned} x(\theta) &= 1 + v(t - 1) \cos \theta, \\ y(\theta) &= v(t - 1) \sin \theta \end{aligned} \quad (5)$$

for $0 \leq \theta \leq \arccos(1/v)$, and the outer part next to the original tumor is given by

$$\begin{aligned} x(\theta) &= t \cos \theta - \beta(t - e^{\theta/\beta}) \sin \theta, \\ y(\theta) &= t \sin \theta + \beta(t - e^{\theta/\beta}) \cos \theta \end{aligned} \quad (6)$$

for $0 \leq \theta \leq \theta_0$. Note that θ appearing in Eqs. (5)–(6) is a parameter, not a polar coordinate.

Figure 3 helps to explain Eqs. (1)–(6). The boundary between the mutant and the original clone moves at constant speed $\beta = \sqrt{v^2 - 1}$, see Fig. 3. Hence the boundary of a mutant clone initiated at $(r, \theta) = (1, 0)$ at time $t = 1$ is described by $r \frac{d\theta}{dr} = \beta$ from which

$$r = e^{\theta/\beta} \quad (7)$$

giving Eq. (1). Equating $t = e^{\theta_0/\beta}$ gives Eq. (2). Setting $\theta_0 = \pi$ yields the capture time (3).

The inner boundary between the mutant clone and the original tumor is given by Eq. (7). The outer boundary of the mutant is composed of two pieces. The first one is a circle (blue curve in Fig. 1) centered at the seed of the mutant clone, i.e., at $(x, y) = (1, 0)$, with radius $R = v[t - 1]$. The opening

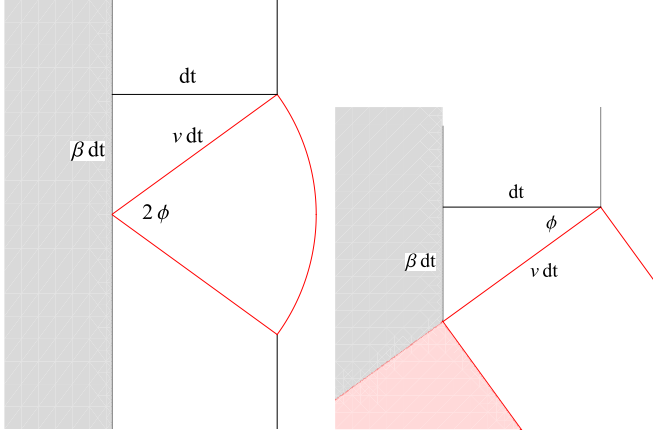


FIG. 3. (Color online) Illustration for the spreading of the mutant clone (a two-dimensional cut is drawn). On the left panel the initiation of a mutant clone is shown. A tiny segment of the surface of the original clone (a shaded region) is almost flat. After a small time interval dt , the surface is composed by a circular arc and straight segments. On the right panel the evolution of the surface of the tumor is shown for later times. The angle ϕ stays constant during the process.

half-angle ϕ of this part of the circle is found by computing the inclination angle between curve (7) and the x axis. One obtains $\phi = \arccos(1/v)$.

To determine the remaining part of the boundary (red curve in Fig. 1) one draws straight lines in the tangential direction from each point of the curve (7) as it is illustrated in Fig. 4. The angle between this tangential and the x axes is ϕ at any point of $r(\theta)$. If we draw the tangential from the point given

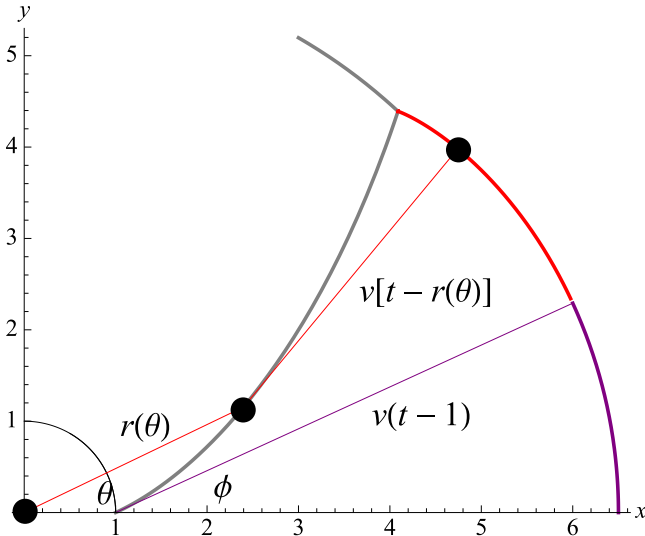


FIG. 4. (Color online) The shape of the mutant clone (only a two-dimensional cut is drawn). The mutant clone is initiated at $(1,0)$. One part of the mutant position is a finite wedge originated from $(1,0)$ with half-angle ϕ and hence the outer boundary being a circle of radius $v(t-1)$. The thick line indicates the boundary of the original tumor, and the curve between the original tumor and the mutant clone is given by the parametric curve $r(\theta)$. The top black dot represents a general point on the outer boundary of the mutant clone. It is reached by the mutant clone originating from the middle black dot in time $t - r(\theta)$ and propagating at speed v .

by polar coordinates $(r(\theta), \theta)$, the mutant clone has still time $t - r$ to grow, so the boundary will be at

$$\begin{aligned} x(\theta) &= r(\theta) \cos \theta + v[t - r(\theta)] \cos[\theta + \arccos(1/v)], \\ y(\theta) &= r(\theta) \sin \theta + v[t - r(\theta)] \sin[\theta + \arccos(1/v)] \end{aligned} \quad (8)$$

which reduce to Eq. (6).

Let us compute the cross-section area of the original tumor at the moment of capture. (Equivalently, the area in the two-dimensional setting). Using Eq. (7) we get

$$A_c = \int_0^\pi d\theta r^2(\theta) = \frac{\beta}{2} (e^{2\pi/\beta} - 1). \quad (9)$$

Similarly one can compute the total cross-section area covered by the tumor (the original tumor and the mutant clone) at the moment of capture:

$$\begin{aligned} A_{\text{tot}} &= \beta^3 (2t_c - \frac{1}{2}) + (\pi + \pi\beta^2 - \frac{3}{2}\beta^3) t_c^2 \\ &\quad + [v(t_c - 1)]^2 \arccos(1/v). \end{aligned} \quad (10)$$

For instance, the term in the bottom line represents the area of the wedge originating at $(1,0)$ with half-angle $\arccos(1/v)$ and the outer boundary being a circle of radius $v(t_c - 1)$.

The ratio A_{tot}/A_c represents the relative enhancement of the area. Perhaps a better characteristic is the ratio

$$\begin{aligned} \frac{A_{\text{tot}}}{A_{\text{no}}} &= 1 + \beta^2 - \frac{1}{2\pi} \beta^3 (1 - t_c^{-1})(3 - t_c^{-1}) \\ &\quad + [v(1 - t_c^{-1})]^2 \frac{\arccos(1/v)}{\pi} \end{aligned} \quad (11)$$

of the total cross-section area covered by the tumor to the area $A_{\text{no}} = \pi t_c^2$ which would be covered by the tumor if there was no mutation. Analysis of Eq. (11) shows that when β increases from 0 to ∞ , the ratio monotonically increases from 1 to $1 + 5\pi^2/6 = 9.22467\dots$

In three dimensions, the calculations are similar. The final volume of the original tumor at the moment of capture is given by the announced expression (4):

$$V_c = \frac{2\pi}{3} \int_0^\pi d\theta \sin \theta r^3(\theta) = \frac{2\pi}{3} \frac{\beta^2}{\beta^2 + 9} (e^{3\pi/\beta} + 1).$$

Note also that the surface area of the original tumor at the moment of capture is

$$\begin{aligned} S_c &= 2\pi \int_0^\pi d\theta \sin \theta r(\theta) \sqrt{r^2(\theta) + \left(\frac{dr}{d\theta}\right)^2} \\ &= \pi v \frac{2\beta}{\beta^2 + 4} (e^{2\pi/\beta} + 1). \end{aligned}$$

The total volume occupied by the tumor at the moment of capture is

$$\begin{aligned} V_{\text{tot}} &= \frac{\pi}{3} \frac{6\beta^4(\beta^2 + 4) - 9\beta^4(\beta^2 + 9)t_c + C(\beta)t_c^3}{\beta^4 + 13\beta^2 + 36} \\ &\quad + \frac{2\pi}{3} (v-1)v^2(t_c-1)^3 \end{aligned} \quad (12)$$

with $C(\beta) = 3\beta^6 + 25\beta^4 + 268\beta^2 + 144$. One can characterize the enhancement of the volume of the tumor at the moment of the capture by dividing the total volume (12) on the volume

$V_{\text{no}} = \frac{4\pi}{3}t_c^3$ which would be covered by the tumor if there was no mutation:

$$\frac{V_{\text{tot}}}{V_{\text{no}}} = \frac{6\beta^4(\beta^2 + 4)t_c^{-3} - 9\beta^4(\beta^2 + 9)t_c^{-2} + C(\beta)}{4(\beta^4 + 13\beta^2 + 36)} + \frac{1}{2}(v-1)v^2(1-t_c^{-1})^3. \quad (13)$$

Analysis of Eq. (13) shows that when β increases from 0 to ∞ , the ratio (13) monotonically increases from 1 to $\frac{\pi^3}{2} + \frac{9\pi^2}{4} - 8 = 29.7097\dots$

IV. PROBABILISTIC ASPECTS

In our simplest model with just one type of mutant cancer cells, distinguishable mutant clones must start on the surface of the original tumor which is not yet covered by mutant clones. The original tumor is eventually captured and no new distinguishable mutant clones will appear after that. Among the simplest probabilistic characteristics are therefore the number of eventual mutant clones, and the times of initiation of mutant clones, which we shall now study for the first two clones. Then we shall explore the fraction of mutant tissue within the tumor with several clones.

A. Arrival time of the first mutant clone

Let T be the arrival time of the first mutant clone, and let us compute the probability $P(T > t)$ that not a single mutant clone has been born during the time interval $(0, t)$. Mutant clones are spontaneously generated at unit rate per unit area of the growing spherical surface, and the surface also grows with unit rate. Hence $P_0(t) = \exp[-\text{volume}]$. The volume of the ball of radius t is $4\pi t^3/3$, so

$$P(T > t) = \exp\left[-\frac{4\pi t^3}{3}\right]. \quad (14)$$

Thus the first mutant arrives with the probability density

$$f(t) = -\frac{dP(T > t)}{dt} = 4\pi t^2 \exp\left[-\frac{4\pi t^3}{3}\right]. \quad (15)$$

The expected value $\mathbb{E}(T) = \int_0^\infty dt t f(t)$ and the variance $\text{Var}(T)$ for the first arrival time are

$$\begin{aligned} \mathbb{E}(T) &= \frac{\Gamma(1/3)}{6^{2/3}\pi^{1/3}} \approx 0.55396, \\ \text{Var}(T) &= \frac{6\Gamma(2/3) - \Gamma(1/3)^2}{6^{4/3}\pi^{2/3}} \approx 0.0405358. \end{aligned}$$

B. Single mutant clone

In Fig. 5, the three-dimensional tumor with a single mutant clone is depicted. Let N be the number of mutant clones originated from the initial tumor. What is the probability $P(N = 1)$ that there is only a single mutant clone from the original clone, so we observe the final barnacle shape of the original tumor. The first mutant clone appears at a random time T , and at distance T from the origin. Conditioning on this time, there are no further mutations with probability

$$P(N = 1|T = t) = e^{-[V_c(\beta) - 4\pi/3]t^3} \quad (16)$$

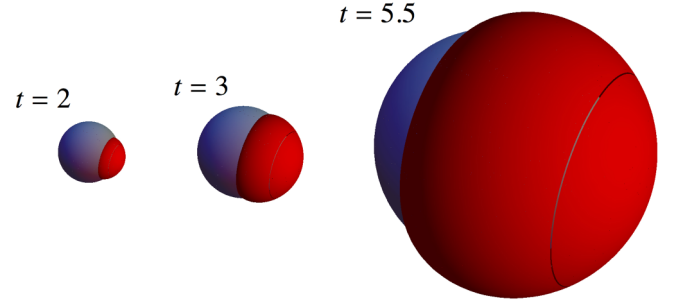


FIG. 5. (Color online) Shape of the tumor with a single mutant clone at times $t = 2, 3$, and 5.5 . The mutant is initiated at $t = 1$ and has fitness $v = 1.5$. The boundary of the mutant clone is red.

since $[V_c(\beta) - 4\pi/3]t^3$ is the total rate of production of the second mutant. Now taking the average over the initiation time, that is averaging over the density $f(t)$ we obtain

$$\begin{aligned} P(N = 1) &= EP(N = 1|T) = 4\pi \int_0^\infty t^2 e^{-V_c(\beta)t^3} dt \\ &= \frac{4\pi}{3V_c(\beta)} = \frac{9 + \beta^2}{\beta^2} \frac{2}{1 + e^{3\pi/\beta}}. \end{aligned} \quad (17)$$

This is the probability that there is exactly one mutant clone, so the original tumor has a final barnacle shape. It is extremely small for realistic relative speeds $v \lesssim 1.4$; it is around 0.36% for $v = 1.5$, and around 3.5% for $v = 2$, although it approaches one as $v \rightarrow \infty$.

C. Arrival of the second mutant clone

We can also calculate the probability distribution of the time of the second mutation. Let T_1 be the time of the first mutation (which is finite with probability one), and let T_2 be the time of the second mutation with $T_2 > T_1$, which is finite with probability $1 - P(N = 1)$. As before, we can write the conditional probability

$$P(T_2/T_1 > \tau | T_1 = t) = e^{-[V(\tau) - 4\pi/3]t^3}, \quad (18)$$

where $1 \leq \tau \leq t_c = e^{\pi/\beta}$, and

$$V(\tau) = 2\pi \frac{\beta^2 + (\beta^2 + 9)\tau^3 + 3\tau^3(\beta \sin \tilde{\theta} + 3 \cos \tilde{\theta})}{3(\beta^2 + 9)}$$

is the volume of the original tumor, with $\tilde{\theta} = \beta \log \tau$. The simplest way to obtain this volume is from its derivative $dV/d\tau = 2\pi\tau^2(1 + \cos \tilde{\theta})$, which is the surface of a sector with half-cone angle $\pi - \theta_0 = \pi - \beta \log \tau$. Now averaging over the arrival time of the first mutant clone we obtain

$$\begin{aligned} P(T_2/T_1 > \tau) &= EP(T_2/T_1 > \tau | T_1) \\ &= 4\pi \int_0^\infty t^2 e^{-V(\tau)t^3} dt = \frac{4\pi}{3V(\tau)} \end{aligned}$$

for $1 \leq \tau \leq e^{\pi/\beta}$. Of course, $P(T_2/T_1 > 1) = 1$, and $P(T_2/T_1 > \tau) = P(N = 1) = \frac{4\pi}{3V_c(\beta)}$ for $\tau \geq t_c = e^{\pi/\beta}$, which corresponds to no second mutation.

D. Spatial characteristics of mutants

Outside of the ball of radius t all tumor cells are mutants, since only mutant tissue grows faster than one. Here we investigate the probability that a random point on distance $r \leq t$ belongs to a mutant.

Consider first the two-dimensional case. Point $(r,0)$ is covered by a mutant initiated at (r_0, θ_0) if this initial point is on or within the boundaries

$$r_0 = r e^{-|\theta_0|/\beta} \quad (19)$$

with $-\pi \leq \theta_0 \leq \pi$. Mutations arrive as an inhomogeneous Poisson process, so we need the total rate of arrival for such a mutation in this region

$$A = \int_0^\pi d\theta [r_0(\theta)]^2 = a(\beta)r^2, \quad a(\beta) = \frac{\beta}{2}(1 - e^{-2\pi/\beta}).$$

Hence the probability of no mutant at distance r in the tumor is

$$W_r = e^{-A} = e^{-a(\beta)r^2}. \quad (20)$$

A random point in the tumor within a disk of radius r , with $r \leq t$, is non-mutant with probability

$$W_{\leq r} = \frac{1}{\pi r^2} \int_0^r dr' 2\pi r' e^{-a(\beta)(r')^2} = \frac{1 - e^{-a(\beta)r^2}}{a(\beta)r^2}. \quad (21)$$

The average non-mutated tumor mass tends to a constant in the large time limit

$$\lim_{t \rightarrow \infty} \pi t^2 W_{\leq t} = \frac{\pi}{a(\beta)}. \quad (22)$$

The calculation is similar in three dimensions. Here, the boundary of points which cover $(r, \theta = 0, \phi = 0)$ is given by the same expression $r_0(\theta)$ as in two dimensions, and the total rate of mutants arriving in this region equals to its volume, which is

$$V = \frac{2\pi}{3} \int_0^\pi d\theta \sin \theta r_0^3(\theta) = b(\beta)r^3 \quad (23)$$

with

$$b(\beta) = \frac{2\pi}{3} \frac{\beta^2}{\beta^2 + 9} (1 + e^{-3\pi/\beta}). \quad (24)$$

At time t , a random point at distance r , with $r \leq t$, is non-mutant with probability $W_r = e^{-V}$. Thus

$$W_r = e^{-b(\beta)r^3}. \quad (25)$$

Further, a random point in a ball of radius r is non-mutant with probability

$$W_{\leq r} = \frac{3}{4\pi r^3} \int_0^r e^{-b(\beta)r'^3} 4\pi r'^2 dr' = \frac{1 - e^{-b(\beta)r^3}}{b(\beta)r^3}.$$

The average non-mutated tumor volume approaches to

$$\lim_{t \rightarrow \infty} \frac{4\pi}{3} t^3 W_{\leq t} = \frac{4\pi}{3b(\beta)} \quad (26)$$

in the large time limit.

Let us check the consistency of Eq. (26) in the extreme case of $v = \infty$. The right-hand side of Eq. (26) is equal to 1 in this limit since $b(\infty) = \frac{4\pi}{3}$ according to Eq. (24). If the mutant

was born at time τ it immediately captures the original tumor when $v = \infty$, so the volume of the original tumor is $\frac{4\pi\tau^3}{3}$. The average volume is $\int_0^\infty d\tau f_1(\tau) \frac{4\pi\tau^3}{3}$ and using Eq. (15) we find it is indeed equal to 1.

V. REDUCTION OF PARAMETERS

Our basic model depends on a single dimensionless parameter, v , the relative growth rate of mutant clones. This is the consequence of a reduction of parameters. Here we discuss how to apply the results if one uses dimension-full units. Let us measure time in days, and distance in cm. In general we have the following parameters describing the system. The surface of the original tumor grows in the normal direction at rate \mathcal{V}_0 , and mutations arrive at the surface of the tumor at rate \mathcal{U} per unit time and unit surface area. The mutant clone growth at rate \mathcal{V}_1 . Let us define the new unit length and time as

$$L_0 = \left(\frac{\mathcal{V}_0}{\mathcal{U}}\right)^{1/3} \quad T_0 = (\mathcal{U}\mathcal{V}_0^2)^{-1/3} = \frac{L_0}{\mathcal{V}_0}.$$

Measuring length and time in these new units, the original clone grows at rate one, and mutations arrive at rate one. The speed of the fronts and mutation rates per surface area might be directly accessible experimentally. Having obtained the unit length and time L_0, T_0 for the tumor, all results of the paper could be used when replacing time with $t \rightarrow t/T_0$ and all lengths with $l \rightarrow l/L_0$. The scaled speed of the mutant clone is

$$v = \mathcal{V}_1/\mathcal{V}_0$$

which is the only parameter of the scaled model.

We can obtain some estimates for the values of the above parameters as follows. In our model the original tumor grows only on the surface as a sphere. Starting from a single cell it reaches volume V_T in time T . In the scaled coordinates the tumor is just a ball of radius scaled time, but here we include explicitly the scaling for the space and time units as given above to obtain

$$\frac{V_T}{L_0^3} = \frac{4\pi}{3} \left(\frac{T}{T_0}\right)^{1/3}.$$

Equivalently, we can rewrite this expression as

$$V_T = \frac{4\pi}{3} (\mathcal{V}_0 T)^3.$$

This gives an estimate for the growth rate

$$\mathcal{V}_0 = \frac{1}{T} \left(\frac{3V_T}{4\pi}\right)^{1/3}.$$

We estimate the surface mutation rate from the number of driver clones found in a tumor. The mean number of clones is $4\pi t^3/3$ in the dimensionless form, or

$$\Lambda_T = \frac{4\pi}{3} \left(\frac{T}{T_0}\right)^{1/3} = \frac{V_T}{L_0^3} = V_T \frac{\mathcal{U}}{\mathcal{V}_0}$$

which then leads to the estimate

$$\mathcal{U} = \frac{\mathcal{V}_0 \Lambda_T}{V_T}.$$

From the above formulas we can obtain an order estimate for our parameters. We expect a tumor of $V_T \approx 1-10 \text{ cm}^3$

after 5 to 10 years of growth (so $T \approx 5-10 \times 365$ day), and we expect of the order of $\Lambda_T \approx 1-10$ driver clones [3,10]. Note that we expect more clones in larger tumors, so roughly

$$\frac{\mathcal{U}}{\mathcal{V}_0} = \frac{\Lambda_T}{V_T} \approx \frac{1}{\text{cm}^3}.$$

This leads to the estimates

$$\mathcal{V}_0 \approx 10^{-3} - 10^{-4} \frac{\text{cm}}{\text{day}}, \quad \mathcal{U} \approx 10^{-3} - 10^{-4} \frac{1}{\text{cm}^2 \text{day}}.$$

Finally, let us estimate the relative speed of the mutant clone $v = \mathcal{V}_1/\mathcal{V}_0$. In [10] it was estimated that the birth rate of cells with k driver mutations is larger by sk than their death rate (that is their fitness is sk), with s being 0.005. If the original clone has k driver mutations, the mutant clone is expected to have $k+1$ mutations. We assume that the speed of a clone is proportional to its fitness advantage, and since everything else is assumed to be the same in the clones, the relative speed of the mutant clone becomes

$$v = \frac{k+1}{k}.$$

Since k is typically an integer between 1 and 8 [3,10], the speed is $1 < v \leq 2$. This is the only parameter of the scaled model.

VI. DISCUSSION

Cancer is a byproduct of evolutionary dynamics among somatic cells of a multi-cellular organism. Cancer arises as cells receive mutations that enable them to escape from control mechanisms and proliferate at higher rates. Most mathematical or computational models of genetic cancer evolution assume well mixed populations of cells without spatial interactions or constraints. This homogeneous setting represents a reasonable framework for the modeling of liquid tumors, but in solid tumors the effects of spatial structure are certainly important.

In this paper, we studied the emergence of driver mutations in a spatial model. Driver mutations enhance the reproductive rate of cancer cells. We assumed that lesions expand roughly with spherical shape. Prior to angiogenesis most cell division occurs on the surface of the expanding tumor. New mutants, which arise on the surface, lead to localized faster growth distorting the spherical shape of the tumor. Our model describes both spatial and temporal evolution and accounts for mutations that activate additional driver genes, leading to enhanced proliferation rates of cancer cells. The model is designed to be as simple as possible, with the basic version depending on the single parameter, the ratio of the growth rates of the mutant clone and the initiating cancer clone. Even in this setting the emerging behavior is rich. For example, the initial clone is inevitably captured by the mutant. Hence the initial clone grows to a fixed size as time goes to infinity. The capture time, however, is much larger than the naive estimate would suggest. This finding correlates with the general conclusion emerging from other studies, see, e.g., [38], namely that spatial structure reduces the rate of cancer progression.

The basic version of our model assumes that there is one type of mutant cells. One can consider n types of mutant cells with fitnesses $1 < v_1 < v_2 \dots < v_n$. Each type is additionally characterized by its birth rate μ_j . We can still set the birth

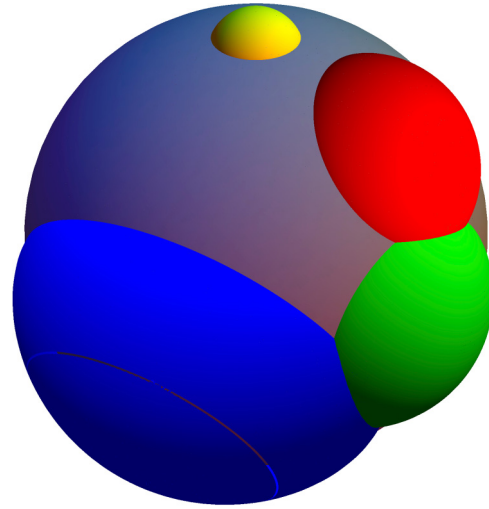


FIG. 6. (Color online) Shape of the tumor with many mutant clones arrived at different times with different fitness values. Mutant clones are initiated stochastically at constant rate on the surface of the original tumor, and then they grow deterministically at constant rate. The growth rates of the mutant clones were chosen randomly between 1 and 2 for this illustration.

rate of the first type of mutant to unity; other birth rates μ_2, \dots, μ_n are parameters of the model. Overall, we have $2n-1$ dimensionless parameters. We should specify where new mutant cells can arise. In the simplest case mutant cells of type $j+1$ can be born only on the growing surface of the mutant clone of type j . The most aggressive mutant of type n eventually captures all other mutants, but the path to this ultimate fate can be very complicated and unpredictable. In Fig. 6 a tumor with multiple mutant clones that have different fitness values is drawn for illustration.

Our model is semi-deterministic—the spatial growth of the tumor is deterministic, while the birth of new mutants is stochastic. The former feature simplifies the analysis. The rules of the dynamics are isotropic: in isolation a mutant clone exhibits a spherical growth. This assumption is realistic and appropriate for describing solid tumors, especially small avascular tumors. Spheroidal shapes are used as a model in anti-cancer therapies [51,60,61]. Yet the stochasticity of the arrival of mutant clones and the strong interaction between the initial clone and mutant clones, and also between different types of mutant clones, results in highly anisotropic shapes.

An important virtue of our model is simplicity. The tractability of the model encourages to pursue its extensions. It would be interesting to study the effect of random growth rates for each mutant clone, the dynamics of new mutant clones arising within mutant clones, and the time it takes to accumulate several additional driver mutations [9,10,13,32,38,62] in a spatial setting.

ACKNOWLEDGMENTS

We thank David Nelson for correspondence. This research was supported by the John Templeton Foundation and the Foundational Questions in Evolutionary Biology Fund.

- [1] B. Vogelstein and W. Kinzler, *The Genetic Basis of Human Cancer* (McGraw-Hill, New York, 1998).
- [2] R. Weinberg, *The Biology of Cancer* (Garland Science, New York, 2013).
- [3] B. Vogelstein, N. Papadopoulos, V. E. Velculescu, S. Zhou, L. A. Diaz, Jr., and K. W. Kinzler, *Science* **339**, 1546 (2013).
- [4] D. Wodarz and N. L. Komarova, *Dynamics of Cancer: Mathematical Foundations of Oncology* (World Scientific, New Jersey, 2014).
- [5] S. H. Moolgavkar and A. G. Knudson, *J. Natl. Cancer Inst.* **66**, 1037 (1981).
- [6] M. A. Nowak, N. L. Komarova, A. Sengupta, P. V. Jallepalli, L.-M. Shih, B. Vogelstein, and C. Lengauer, *Proc. Natl. Acad. Sci. USA* **99**, 16226 (2002).
- [7] N. L. Komarova, A. Sengupta, and M. A. Nowak, *J. Theor. Biol.* **223**, 433 (2003).
- [8] M. A. Nowak, F. Michor, N. L. Komarova, and Y. Iwasa, *Proc. Natl. Acad. Sci. USA* **101**, 10635 (2004).
- [9] N. Beerenwinkel, T. Antal, D. Dingli, A. Traulsen, K. W. Kinzler, V. E. Velculescu, B. Vogelstein, and M. A. Nowak, *PLoS Comput. Biol.* **3**, e225 (2007).
- [10] I. Bozic, T. Antal, H. Ohtsuki, H. Carter, D. Kim, S. Chen, R. Karchin, K. W. Kinzler, B. Vogelstein, and M. A. Nowak, *Proc. Natl. Acad. Sci. USA* **107**, 18545 (2010).
- [11] C. D. McFarland, K. S. Korolev, G. V. Kryukov, S. R. Sunyaev, and L. A. Mirny, *Proc. Natl. Acad. Sci. USA* **110**, 2910 (2013).
- [12] C. D. McFarland, L. A. Mirny, and K. S. Korolev, *Proc. Natl. Acad. Sci. USA* **111**, 15138 (2014).
- [13] S. Yachida, S. Jones, I. Bozic, T. Antal, R. Leary, B. Fu, M. Kamiyama, R. H. Hruban, J. R. Eshleman, M. A. Nowak, V. E. Velculescu, K. W. Kinzler, B. Vogelstein, and C. A. Iacobuzio-Donahue, *Nature* **467**, 1114 (2010).
- [14] N. L. Komarova and D. Wodarz, *Proc. Natl. Acad. Sci. USA* **102**, 9714 (2005).
- [15] F. Michor, T. P. Hughes, Y. Iwasa, S. Branford, N. P. Shah, C. L. Sawyers, and M. A. Nowak, *Nature* **435**, 1267 (2005).
- [16] Y. Iwasa, M. A. Nowak, and F. Michor, *Genetics* **172**, 2557 (2006).
- [17] N. L. Komarova, *J. Theor. Biol.* **239**, 351 (2006).
- [18] I. Bozic *et al.*, *eLife* **2**, e00747 (2013).
- [19] N. Beerenwinkel, R. F. Schwarz, M. Gerstung, and F. Markowetz, *System. Biol.* **64**, E1 (2015).
- [20] H. M. Byrne, T. Alarcon, M. R. Owen, S. D. Webb, and P. K. Maini, *Phil. Trans. R. Soc. A* **364**, 1563 (2006).
- [21] J. A. Sherratt and M. A. Nowak, *Proc. R. Soc. Lond. B* **248**, 261 (1992).
- [22] T. Roose, S. J. Chapman, and P. K. Maini, *SIAM Rev.* **49**, 179 (2007).
- [23] M. M. Baraldi, A. A. Alemi, J. P. Sethna, S. Caracciolo, C. A. M. La Porta, and S. Zapperi, *J. Stat. Mech.* (2013) P02032.
- [24] B. Perthame, F. Quirós, and J. L. Vázquez, *Arch. Ration. Mech. Anal.* **212**, 93 (2014).
- [25] Y. Jiao and S. Torquato, *PLoS Comput. Biol.* **7**, e1002314 (2011).
- [26] G. De Matteis, A. Graudenzi, and A. M. Antonietti, *J. Math. Biol.* **66**, 1409 (2013).
- [27] A. Friedman, in *Lecture Notes in Mathematics*, Vol. 1872 (Springer-Verlag, Berlin, 2006), p. 223.
- [28] H. M. Byrne and M. A. J. Chaplain, *Euro. J. Appl. Math.* **8**, 639 (1997).
- [29] S. Cui and A. Friedman, *J. Math. Anal. Appl.* **255**, 636 (2001).
- [30] A. Sottoriva, *Proc. Natl. Acad. Sci. USA* **110**, 4009 (2012).
- [31] A. M. Klein, D. P. Doupé, P. H. Jones, and B. D. Simons, *Phys. Rev. E* **76**, 021910 (2007).
- [32] R. Durrett and S. Moseley, *Theor. Popul. Biol.* **77**, 42 (2010).
- [33] T. Antal and P. L. Krapivsky, *J. Stat. Mech.* (2011) P08018.
- [34] C. A. M. La Porta, S. Zapperi, and J. P. Sethna, *PLoS Comput. Biol.* **8**, e1002316 (2012).
- [35] T. Williams and R. Bjerknes, *Nature* **235**, 19 (1972).
- [36] M. Bramson and D. Griffeath, *Math. Proc. Cambridge Philos. Soc.* **88**, 339 (1980).
- [37] M. Bramson and D. Griffeath, *Ann. Probab.* **9**, 173 (1981).
- [38] E. A. Martens, R. Kostadinov, C. C. Maley, and O. Hallatschek, *New J. Phys.* **13**, 115014 (2011).
- [39] A. R. Kansal, S. Torquato, E. A. Chiocca, and T. S. Deisboeck, *J. Theor. Biol.* **207**, 431 (2000).
- [40] B. Waclaw, I. Bozic, M. E. Pittman, R. H. Hruban, B. Vogelstein, and M. A. Nowak, *arXiv:1503.07116*.
- [41] N. L. Komarova, *Math. Biosci. Eng.* **10**, 3 (2013).
- [42] M. A. Nowak, F. Michor, and Y. Iwasa, *Proc. Natl. Acad. Sci. USA* **100**, 14966 (2003).
- [43] R. Durrett and S. Moseley, *Ann. Appl. Probab.* **25**, 104 (2015).
- [44] J. W. Evans, *Rev. Mod. Phys.* **65**, 1281 (1993).
- [45] M. Kleban, *Class. Quantum Gravity* **28**, 204008 (2011).
- [46] R. M. Bradley and P. N. Strenski, *Phys. Rev. B* **40**, 8967 (1989).
- [47] Yu. A. Andrienko, N. V. Brilliantov, and P. L. Krapivsky, *Phys. Rev. A* **45**, 2263 (1992).
- [48] I. G. Ron, I. Golding, B. Lifshitz-Mercer, and E. Ben-Jacob, *Physica A* **320**, 485 (2003).
- [49] O. Hallatschek and D. R. Nelson, *Evolution* **64**, 193 (2010).
- [50] K. S. Korolev, M. J. I. Müller, N. Karahan, A. W. Murray, O. Hallatschek, and D. R. Nelson, *Phys. Biol.* **9**, 026008 (2012).
- [51] F. Hirschhaeuser *et al.*, *J. Biotechnology* **148**, 3 (2010).
- [52] J. H. van Es and H. Clevers, *Methods Mol. Biol.* **1267**, 125 (2015).
- [53] A. Brú, S. Albertos, J. L. Subiza, J. L. García-Asenjo, and I. A. Brú, *Biophys. J.* **85**, 2948 (2003).
- [54] A. Brú, S. Albertos, J. A. López García-Asenjo, and I. Brú, *Phys. Rev. Lett.* **92**, 238101 (2004).
- [55] D. Drasdo and S. Höhme, *Phys. Biol.* **2**, 133 (2005).
- [56] M. A. J. Chaplain, M. Ganesh, and I. G. Graham, *J. Math. Biol.* **42**, 387 (2001).
- [57] P. Ciarletta, D. Ambrosi, G. A. Maugin, and L. Preziosi, *Eur. Phys. J. E* **36**, 23 (2013).
- [58] M. O. Lavrentovich and D. R. Nelson, *Theor. Popul. Biol.* **102**, 26 (2015).
- [59] T. A. Cook, *The Curves of Life* (Dover, London, 1985).
- [60] L. A. Kunz-Schughart, *Cell Biol. Int.* **23**, 157 (1999).
- [61] A. Lorz, T. Lorenzi, J. Clairambault, A. Escargueil, and B. Perthame, *Bull. Math. Biol.* **77**, 1 (2015).
- [62] S. Jones, W. Chen, G. Parmigiani, F. Diehl *et al.*, *Proc. Natl. Acad. Sci. USA* **105**, 4283 (2008).